RSC Advances

PAPER

View Article Online
View Journal | View Issue

Cite this: *RSC Adv.*, 2025, **15**, 7354

A sustainable framework for advancing circular practices for polyethylene terephthalate textiles: optimized recycling of depolymerization byproducts and LCA validation†

Ye-eun Woo,[a] Kyungha Baik,[a] Sujin Jeong,[a] Suhyun Lee [ab] and Jooyoun Kim *[ab]

This study demonstrates a novel circular approach for discarded polyethylene terephthalate (PET) textiles with life cycle assessment (LCA) validation, proposing an optimized recycling method for PET depolymerization byproducts. The experimental approach emphasizes sourcing the metal–organic framework ingredients including metal and linker components from a single PET depolymerization reaction. For depolymerization, a metal salt-based deep eutectic solvent (DES) composed of *p*-toluene sulfonic acid and iron(III) chloride hexahydrate was employed acting as both solvent and catalyst. Sequential recovery processes for multiple depolymerization products were established, and their recyclability was demonstrated. LCA was performed on the varied scenarios of the developed process, and the results provided solid grounds to conclude that the suggested process produces relatively less burden on the environment, attributed to the effective catalytic action of DES and the maximized use of byproducts generated from the depolymerization reactions. This work pioneers a comprehensive approach integrating novel experimental methods with LCA validation, establishing a robust proof-of-concept for maximizing the recycling potential of PET depolymerization products.

Received 24th January 2025
Accepted 3rd March 2025

DOI: 10.1039/d5ra00572h

rsc.li/rsc-advances

Introduction

Metal–organic frameworks (MOFs), composed of inorganic metal nodes and organic linkers, have drawn rising attention in a wide range of applications including foulant adsorption, drug delivery, photocatalysis, gas separation and storage due to their high porosity, large surface area, adjustable pore size, and chemical tailorability.[1–3] Among the numerous organic linkers forming MOFs, terephthalic acid (TA, or benzenedicarboxylic acid, BDC) or bis(2-hydroxyethyl) terephthalate (BHET) are well suited to construct useful MOFs including HKUST-1, UiO-66, and MIL-88B, which exhibit notable stability in aqueous environments and serve as effective adsorbents for pollutant removal.[4–7] Since TA is one of the monomeric constituents of polyethylene terephthalate (PET), which comprises the largest proportion of synthetic textile materials, using PET waste as a source of MOF linkers has been explored as a green synthesis strategy to solve fiber waste pollution by producing high-value products.[8–12]

Regarding PET depolymerization, various methods have been suggested toward efficient and eco-friendly processes to lower the environmental burden such as process temperature, time, and byproduct waste.[13–15] Most of the prior studies employed catalysts to reduce the activation energy in the depolymerization reaction.[16–23] With the catalytic effect of metal salts, metal salt-based deep eutectic solvents (DES) have gained attention.[24,25] DES is a mixture of two or three-component chemicals, which are associated with hydrogen bonds to form a liquid with a single melting point lower than the individual components. When the metal salt-based DES is used as a solvent for PET depolymerization, the chain disassociation is accelerated by the synergistic effect, whereby the metal salt acts as a Lewis acid and the other component acts as a Brønsted acid. Despite the benefit of metal-based DES, they often leave the unwanted metal complex and byproducts in the reaction system, contaminating the solvent.[26,27] Therefore, measures to effectively remove and/or utilize the generated metal byproducts need to be studied to overcome the current challenges of using metal-based catalysts in a depolymerization system.

Most of the prior studies for PET-derived MOF synthesis were performed for (1) obtaining a high-purity TA from depolymerization of uncolored PET plastic bottles or textiles, and (2)

[a]*Department of Fashion and Textiles, Seoul National University, Seoul 08826, Republic of Korea. E-mail: jkim256@snu.ac.kr*

[b]*Research Institute of Human Ecology, Seoul National University, Seoul 08826, Republic of Korea*

† Electronic supplementary information (ESI) available. See DOI: https://doi.org/10.1039/d5ra00572h

synthesizing a well-defined MOF of interest. While numerous studies have progressed in this area, most of earlier studies have rarely paid attention to the discarded byproducts generated from the depolymerization process other than TA, and the metal nodes of MOF were still sourced from commercially purchased materials. As a prior attempt to source both metal and ligand components from waste, Song *et al.*[28] sourced the metal node and TA from the nickel-containing electroplating sludge (EPS) and PET waste, respectively, and synthesized Ni-MOF. While this study demonstrated a way to source the main MOF ingredients from the waste, it involved independent processes to extract the metal and ligand ingredients from each EPS and PET, which may require high cost and environmental burden due to the complex processes. Therefore, to conceive a significantly sustainable recycling strategy, it is essential to account for simple and environmentally responsible processes with minimized generation of process byproducts and waste.

Herein, a novel strategy of recycling the TA and reaction byproducts from PET depolymerization is suggested by developing a series of processes to extract and separate TA (or TA in NaOH aq. solution), metal compounds, and dye, as shown in Fig. 1. A particular emphasis lies in sourcing the MOF ingredients including both metal and linker components from a single reaction system of PET depolymerization. Furthermore, dye from the discarded PET fabric was also simultaneously recovered from the depolymerization system, and it was recycled for dyeing an uncolored PET fabric. Aiming at developing an environmentally responsible PET depolymerization process, a metal salt-based DES, comprised of *p*-toluene sulfonic acid (PTSA) and iron(III) chloride hexahydrate ($FeCl_3 \cdot 6H_2O$), was employed for an efficient reaction with lowered temperature and time. Sequential processes of recovering TA, $FeCl_3 \cdot 6H_2O$, and dye from the reaction solution were developed, and a series of recycling approaches were developed for: recycling TA and $FeCl_3$ for the synthesis of MIL-88B(Fe), and recycling the dye.

Life cycle assessment (LCA) was performed on the developed depolymerization process and the suggested process was compared to others from prior studies.[29,30] Furthermore, LCA was tested for varied scenarios in which certain byproducts were credited as useful byproducts. The LCA results provided solid grounds to conclude that the developed process produces relatively less burden on the environment, attributed to the effective catalytic action of DES and the optimized use of byproducts. This study offers an innovative circular strategy for discarded PET by conceiving a series of sequential processes to recover reaction byproducts and by recycling them. To our knowledge, it is the first time to report a comprehensive discussion including the novel experimental approach and the LCA validation. The significance of this study lies in demonstrating a novel proof-of-concept recycling approach and offering an integrated assessment method to substantiate the experimental results. Ultimately, this study contributes to a sustainable framework for advancing circular practices in PET recycling.

Materials and methods

Materials

Undyed PET fabric was purchased from Testfabrics, Inc. (USA), and discarded dyed PET fabric was obtained elsewhere. Iron(III) chloride hexahydrate ($FeCl_3 \cdot 6H_2O$), *p*-toluene sulfonic acid (PTSA), terephthalic acid (TA), hydrochloric acid (HCl), sodium hydroxide (NaOH), *N*,*N*-dimethylformamide (DMF), and ethanol were purchased from Daejung Chemicals (Korea) and used without further purification. Rhodamine B (RhB) was supplied by SCI Seoul Chemical (Korea).

PET depolymerization

The DES was synthesized by heating a mixture of $FeCl_3 \cdot 6H_2O$ and PTSA at 60 °C until a homogeneous dark red liquid was obtained. PET fabrics were cut into 1 cm × 1 cm pieces, and 5 g of fabric pieces were immersed in 25 g of DES. The mixture was heated at varied reaction temperatures (80, 90, 100, and 110 °C) for varied reaction times (15, 30, 45, and 60 min) to determine the optimal depolymerization condition.

After the depolymerization reaction, powdery TA, iron oxides, extracted dyes, and PET fragments with incomplete degradation were precipitated in DES solution. These precipitates were separated from the DES solution by passing through a glass filter (pore size of 15–40 μm) at least twice. Among the

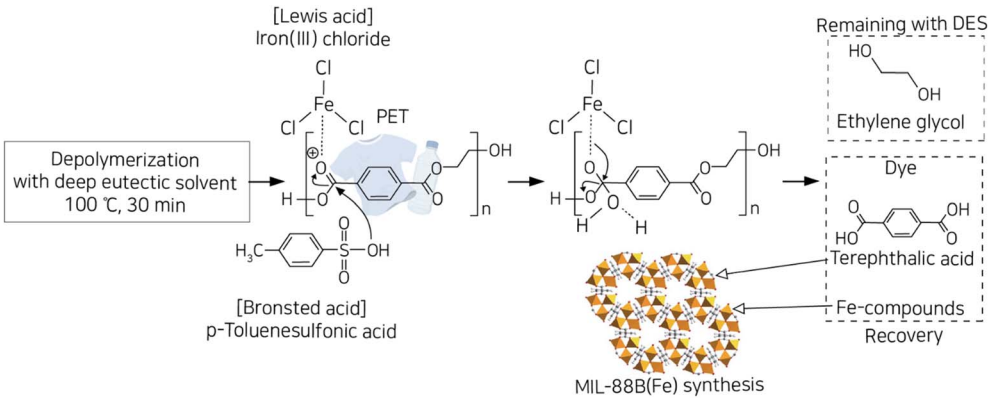

Fig. 1 Schematic overview of processes for PET depolymerization with catalytic activity of DES, chemicals recovery, and MOF synthesis.

separated precipitates, visibly apparent PET fragments were easily removed. After cleaning the PET fragments, their weight was measured as W'_{PET}. The remaining precipitates, which were TA, Fe-compound, and dyes, were mixed with 20 mL of 2 M NaOH aq. solution to selectively dissolve the TA. Fe-compound and dyes were filtered out of a glass filter (pore size of 15–40 μm), leaving TA/NaOH eluent. This TA/NaOH solution was used as is for MOF synthesis step without further purification.

To calculate TA yield (%) and crystal analysis, it was necessary to obtain TA solid particles. For this, 8 mL of 10 M HCl aq. solution was added to the TA/NaOH solution to sediment TA precipitate and NaCl. After NaCl was removed by washing with distilled water, high-purity TA particles were collected. The depolymerization efficiency (%) and TA yield (%) for varied process conditions were calculated using eqn (1) and (2); where W_{PET} is the weight of PET fabric, W'_{PET} is the weight of PET fragments with incomplete degradation, and W_{TA} is the weight of TA obtained from the reaction.[31] The coefficient of 0.85 represents the theoretical ratio of the molecular weight of TA units ($C_8H_4O_4$, 164.11 g mol^{-1}) to that of ethylene terephthalate repeating units ($C_{10}H_8O_4$, 192.17 g mol^{-1}).[32]

$$\text{Depolymerization efficiency}(\%) = \frac{W_{PET} - W'_{PET}}{W_{PET}} \times 100 \quad (1)$$

$$\text{TA yield}(\%) = \frac{W_{TA}}{W_{PET} \times 0.85} \times 100 \quad (2)$$

The remaining precipitates of Fe-compound and dyes were mixed with 4 mL of 10 M HCl aq. solution. At this time, the Fe-compound was dissolved in aq. HCl solution, presumably forming $FeCl_3 \cdot 6H_2O$, whereas the dye is precipitated. The dye particles were separated by the glass filter and dried. This dye was recycled later for dyeing the uncolored PET fabric. The Fe-compound (presumably $FeCl_3 \cdot 6H_2O$) in 10 M HCl aq. solution was concentrated to about 60 wt%, evaporating the solvent at 100 °C, and 14 mL of concentrated solution was stored at 5 °C to precipitate $FeCl_3 \cdot 6H_2O$.

Synthesis of MIL-88B(Fe)

The TA dissolved in 2 M NaOH aq. solution and $FeCl_3 \cdot 6H_2O$ (s), which were recovered from PET depolymerization process, were used for MIL-88B(Fe) synthesis. A 0.635 g of $FeCl_3 \cdot 6H_2O$ and 4 mL of TA/NaOH aq. solution were added in 50 mL of DMF under sonication. The solution was then placed in a hydrothermal reactor and heated at 100 °C for 12 h. The resulting MIL-88B(Fe) was washed with DMF and ethanol, and then oven-dried at 60 °C for 24 h for activation.

Characterization

Thermal property of dyed PET sample was examined by differential scanning calorimetry (DSC) (DSC Q100, Ta Instruments, USA) with heating and cooling rates of 5 °C min^{-1} under nitrogen (N_2) gas flow (50 mL min^{-1}). The precipitated Fe-containing compound was analyzed for its composition by the wavelength dispersive X-ray fluorescence spectrometer (WD-XRF) (ZSX Primus, Rigaku, Japan). The collected TA and dye were analyzed by the Fourier transform infrared assembled with attenuated total reflectance spectroscopy (FT-IR) (Vertex-80V, Bruker Corp., Germany). Morphology of MIL-88B(Fe) was observed by a field-emission scanning electron microscopy (FE-SEM) (JSM-7800F Prime, JEOL Ltd, Japan) with prior Pt-coating using a sputter coater (108 Auto Sputter Coater, Ted Pella, USA). The crystalline phase of MIL-88B(Fe) was analyzed using X-ray diffraction (XRD) (SmartLab, Rigaku Corp., Japan) with a Cu-targeted X-ray generator. Brunauer–Emmett–Teller (BET) adsorption analysis was conducted for MIL-88B(Fe) by the nitrogen (N_2) sorption–desorption isotherm (Tristar ll 3020, Micromeritics, USA).

Adsorption property of MIL-88B(Fe)

The adsorption performance of MIL-88B(Fe) was examined using RhB dye as a model water pollutant. In this test, 0.015 g of MIL-88B(Fe) was immersed in 50 mL of aq. dye solution (20 mg L^{-1}), and the concentration of RhB solution was measured over time. The dye concentration was determined by measuring the absorbance at 553 nm of RhB using a multi-mode microplate reader (BioTek Synergy H1, Agilent, USA).

Dyeing performance of recycled dye

A 2 g of uncolored PET fabric was treated with 100 mL of 0.8 g L^{-1} dye solution (4% on the weight of fabric), in which the dye was the one recovered from PET depolymerization process. The pH of the dyeing solution was adjusted to 4.5 using acetic acid, and the dyeing procedure was conducted at 130 °C for 1 h, followed by washing with distilled water to remove unfixed dyes. The color of the fabric dyed with the recycled dye was compared with that of the originally dyed PET fabric before depolymerization, using the CIE L^* a^* b^* color system. The color difference between the samples ΔE was calculated as eqn (3). In this eqn, L^* indicates the lightness of the sample, a^* indicates the redness/greenness, and b^* indicates yellowness/blueness. The ΔL^*, Δa^*, and Δb^* represent the lightness and color difference between the originally dyed PET sample and the PET dyed with recycled dye. The L^*, a^*, b^* measurements were done at least five times.

$$\Delta E = \sqrt{(\Delta L^*)^2 + (\Delta a^*)^2 + (\Delta b^*)^2} \quad (3)$$

Life cycle assessment

LCA was performed on the processes including PET depolymerization and the byproduct recovery. The system boundary of the LCA was defined as 'cradle-to-gate' including transport (Fig. S7†). To perform LCA, the 'cut-off' method was applied. Ecoinvent version 3.10 database and OpenLCA software version 2.3.0 were used to implement LCA. ReCiPe 2016 version 1.03 (Hierarchist) method was utilized to calculate the impact categories. The functional unit of 1 kg sorted waste PET was inserted into the depolymerization process. The assumptions applied to accomplish the LCA are summarized in Table S2.†

The scenarios analyzed in this research are summarized in Table S3.† The input and output data were calculated from lab-scale data of this work, which recycled 5 g of PET (Tables S4–S6†). This LCA aimed to find major contributors to impacts and suggest a better scenario for further research and industrialization. The detailed information for LCA implementation including assumptions, inputs, outputs, inventories, and providers is summarized in ESI Section 2.†

Results and discussion

Optimization of PET depolymerization

As shown in eqn (1), PET depolymerization efficiency (%) was defined as the extent to which PET was depolymerized into smaller molecular chains until the apparent fiber pieces were not observed. The depolymerization of various PET-based materials, including PET bottles and fibers, using $FeCl_3 \cdot 6H_2O$/PTSA confirmed that the solvent effectively depolymerizes PET (Table S1†). In Fig. 2, depolymerization efficiency (%) and TA yield (%) of dyed PET were examined with respect to reaction parameters, including the PET to DES mass ratio, the molar ratio of $FeCl_3 \cdot 6H_2O$ to PTSA, process time and temperature. Fig. 2a shows the depolymerization efficiency as a function of PET to DES (solvent and catalyst) mass ratio when the reaction was carried out at 100 °C for 30 min in DES with a molar ratio of $FeCl_3 \cdot 6H_2O$ to PTSA of 1 : 1. When PET DES mass ratio was 1 : 3, the amount of solvent was insufficient to fully immerse the PET mass (Fig. S1†), inhibiting the proper depolymerization. As the PET DES mass ratio increased to 1 : 5 or higher, PET was sufficiently immersed in DES, reaching 100% depolymerization efficiency and 95% TA yield. Thus, the optimized mass ratio of PET to DES was determined to be 1 : 5.

Fig. 2b shows the depolymerization efficiency and TA yield with varied molar ratios of $FeCl_3 \cdot 6H_2O$ to PTSA when the experiment was conducted at 100 °C for 30 min with a PET to DES mass ratio of 1 : 5. The $FeCl_3 \cdot 6H_2O$ or PTSA alone was in the solid phase, thus, neither could be used as a solvent. To test the depolymerization efficiency by the single component-solvent ($FeCl_3 \cdot 6H_2O$ PTSA of 1 : 0 or 0 : 1), an 80% aqueous solution of either $FeCl_3 \cdot 6H_2O$ or PTSA was prepared. In either case of $FeCl_3 \cdot 6H_2O$ or PTSA aq. solution, PET fabrics remained intact with 0% depolymerization efficiency. Yang *et al.*[33] reported that PET was depolymerized by PTSA solution (80%) at 150 °C within 90 min, but under the conditions of this experiment at 100 °C for 30 min, depolymerization was very limited. When a DES with $FeCl_3 \cdot 6H_2O$ and PTSA was used as the solvent, 100% depolymerization efficiency and 95% TA yield were attained at 100 °C, regardless of the molar ratios tested in this study. In the depolymerization process, $FeCl_3 \cdot 6H_2O$ acts as a Lewis acid by accepting electron pairs from the oxygen in the ester bonds, and it weakens the ester linkage. In the meanwhile, PTSA acts as a Brønsted acid by donating H^+ ions and cleaves the ester bonds.[34] By the dual activation of PTSA and $FeCl_3 \cdot 6H_2O$, the reaction is facilitated, allowing the depolymerization at a lower temperature. After the reaction, a partial amount of $FeCl_3 \cdot 6H_2O$ was precipitated and it was recovered by the subsequent process to be used for MOF synthesis. As the amount of $FeCl_3 \cdot 6H_2O$ in DES gradually reduced with

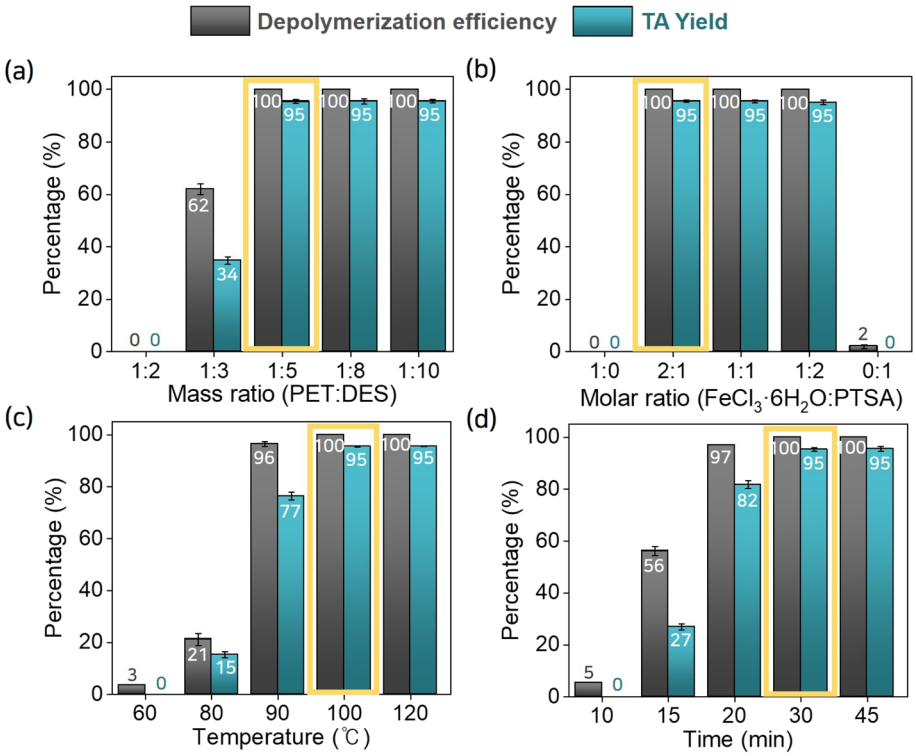

Fig. 2 Depolymerization efficiency and TA yield with varied conditions. (a) PET to DES mass ratio, (b) $FeCl_3 \cdot 6H_2O$ to PTSA molar ratio, (c) reaction temperature, and (d) reaction time.

precipitation, the molar ratio of 2 : 1, with a higher ratio of $FeCl_3 \cdot 6H_2O$, was chosen as an optimal condition, in consideration of recycling the DES for the next PET depolymerization.

The optimal reaction temperature was examined in Fig. 2c, fixing the other process conditions as follows; PET DES mass ratio of 1 : 5, $FeCl_3 \cdot 6H_2O$ PTSA molar ratio of 2 : 1, reaction time 30 min). At 80 °C, only 20% of PET depolymerization was attained. The glass transition temperature (T_g) of the dyed PET sample, analyzed by DSC, was approximately 85 °C (Fig. S2†). This suggests that polymer chains will have segmental motions above this temperature, at least in the amorphous region, allowing efficient DES penetration into the polymer chains. For that reason, a substantial portion of PET began to depolymerize from 90 °C onward, and at 100 °C and above, about 95% TA yield was attained. From Fig. 2d, under the optimized conditions (PET DES of 1 : 5, $FeCl_3 \cdot 6H_2O$ PTSA of 2 : 1, 100 °C), a minimum reaction time of 30 min of reaction time was required to achieve a 95% TA yield. A longer reaction time did not contribute to a higher TA yield. The discrepancy between depolymerization efficiency and TA yield at 15 min reaction time demonstrates that the random hydrolysis reaction occurs first, producing shorter chains and oligomers, and as the degradation proceeds, it further degrades to TA and ethylene glycol (EG).

This study aimed to design a PET depolymerization process with minimal environmental impacts with lower reaction temperature, less reaction time, and less use of solvent. By using DES as a solvent, the reaction temperature was lowered compared to that of conventional acid or alkaline hydrolysis. The optimal depolymerization condition for obtaining 95% TA yield (%) was chosen as 1 : 5 PET to DES ratio, 2 : 1 $FeCl_3 \cdot 6H_2O$ to PTSA, 100 °C reaction temperature, and 30 min reaction time, and those process parameters were employed for later experiments. The comparative LCA of the depolymerization process is discussed further in the later section.

Byproduct recovery

In the depolymerization reaction, precipitates including TA, dye from PET fabric, and Fe-compound from $FeCl_3 \cdot 6H_2O$ were formed in the solution. Each component of the precipitates was separated and recovered as described in the 'methods' section. When the precipitates were added to a 2 M of aq. NaOH solution, only TA dissolved, while the dye and Fe-impurities remained as solid precipitates. The TA/NaOH solution was separated and then the solution was directly used for the synthesis of MIL-88B(Fe) without further purification of TA. To confirm the presence of TA in the NaOH solution (denoted as 'recovered TA/NaOH'), FT-IR analysis was performed on the TA/NaOH solution, and the resulting peaks were compared with those of commercially purchased TA dissolved in 2 M of aq. NaOH solution (denoted as 'commercial TA/NaOH'). From Fig. 3, the FT-IR peaks of recovered TA/NaOH matched those of commercial TA/NaOH, presenting: 3440 cm^{-1} for OH stretching due to hydrogen bonding with hydroxide ions (OH^-);[35] 1652 cm^{-1} for C=O stretching;[36,37] 1580 cm^{-1} for C=C of the benzene ring;[37,38] 1411 for OH in-plane deformation.[39] From the

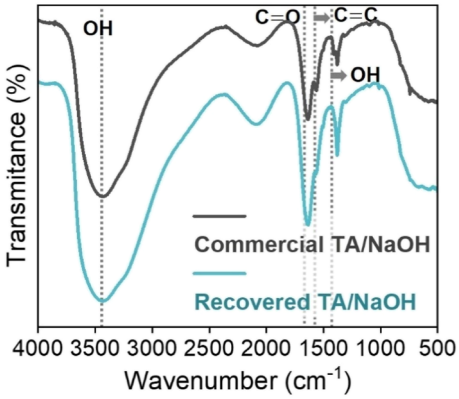

Fig. 3 FT-IR spectra of recovered TA/NaOH and commercial TA/NaOH.

UV absorbance in Fig. S3,† the commercial TA (purity >97%) and the recovered TA showed a similar trend with varying concentrations. While an exact purity of the recovered TA was not analyzed, the experiment suggests the recovered TA has a purity as close to the commercial one.

The remaining precipitates after TA separation were analyzed by XRF (Table 1) to examine the compositions. From the analysis, the precipitates contained 80 wt% Fe in the Fe_2O_3 form; Cl and SO_3 from the dyes of PET fabric;[40,41] and TiO_2, a common pigment added in PET fiber manufacturing.[42–44] The Fe_2O_3 was generated through the following process. When PET was depolymerized in DES, TA precipitated, binding with Fe^{3+} ions in the solution. The Fe^{3+} containing precipitate reacts with OH^- of NaOH solution, and $Fe(OH)_3$ (s) is precipitated. Subsequently, $Fe(OH)_3$ is oxidized to Fe_2O_3 in the air,[45] and Fe_2O_3 remains as a solid byproduct.

$$Fe^{3+} + 3OH^- \rightarrow Fe(OH)_3\,(s)\downarrow$$

$$4Fe(OH)_3 + 3O_2 \rightarrow 2Fe_2O_3 + 12\,OH^-$$

The precipitates consisting of Fe_2O_3 and dye are typically treated as reaction waste; however, in this study, Fe_2O_3 was reacted with HCl aq. solution to produce $FeCl_3 \cdot 6H_2O$, which was then used for the synthesis of MIL-88B(Fe). When the precipitates containing Fe_2O_3 and dye were treated with HCl aq. solution, only dye precipitated. After the dye was separated by filtration, it was recycled for dyeing an uncolored PET fabric. For the recovered crystals of $FeCl_3 \cdot 6H_2O$,[46] the morphology and elemental compositions were analyzed by SEM-EDS (Fig. S4†),

Table 1 XRF analysis of Fe-containing precipitates

Oxide	
Component	Mass (%)
Fe_2O_3	80
Cl	12
SO_3	5
TiO_2	3

where the atomic ratio of Fe Cl was found to be about 1 : 3. The XPS analysis of Fig. 4a–c was performed to verify the hydration status of $FeCl_3$. In Fig. 4a, the peak at the binding energy of 710.97 eV and 724.07 eV were attributed to Fe(III) $2p_{3/2}$ and Fe(III) $2p_{1/2}$, while the peak at 715.12 eV and 729.47 eV corresponded to the satellite peak of Fe(III) $2p_{3/2}$ and Fe(III) $2p_{1/2}$.[47,48] In Fig. 4b, Fe–Cl bonds and Cl $2p_{1/2}$ at binding energies of 198.6 and 200.6 eV.[49,50] In Fig. 4c, the presence of H_2O was observed at 532.3 eV and O–Fe at 533.4 eV.[51,52] The XRD analysis shown in Fig. 4d supports the identical crystal structures of $FeCl_3 \cdot 6H_2O$ and r-$FeCl_3 \cdot 6H_2O$ with distinct peaks at 15.2°, 20.1°, 25.38°, 28.18°, 36.8°, 46.48° and 50.56°.[53] This confirms the successful recovery of $FeCl_3 \cdot 6H_2O$ in the PET recycling process. The recycled $FeCl_3 \cdot 6H_2O$ could be used as an addition to the DES component, but we used it as a source of metal component for MIL-88B(Fe) synthesis. Although the purity of the recycled $FeCl_3 \cdot 6H_2O$ was not directly calculated, it exhibited XRD peaks very similar to those of commercially purchased $FeCl_3 \cdot 6H_2O$, and the successful synthesis of the MOF suggests that a high yield of $FeCl_3 \cdot 6H_2O$ was obtained.

After the 1st depolymerization (dep'n) process with the subsequent byproduct recovery, the remaining DES solution was recycled for the 2nd PET dep'n. It is noted that after the 1st dep'n, EG was not separated from the DES solution. Thus, the DES reused for the 2nd dep'n certainly contains EG; however, in this case, EG remaining in DES may be beneficial as functions as a catalyst for PET dep'n.[54,55] For the 2nd dep'n experiment, 5 g of discarded PET fabric was reacted with the recycled DES solvent, and it produced the same depolymerization efficiency (100%) and TA yield (95%) as the 1st dep'n reaction (Fig. S5†). This result demonstrates the efficient recyclability of DES at least in the 2nd dep'n process.

MIL-88B(Fe) synthesis with recycled compounds

The TA/NaOH and $FeCl_3 \cdot 6H_2O$ obtained from the PET depolymerization process were used for the synthesis of MIL-88B(Fe), which is denoted as r-MIL-88B(Fe). The characteristics of r-MIL-88B(Fe) were compared with those of MIL-88B(Fe) synthesized from commercial chemicals of TA, $FeCl_3 \cdot 6H_2O$ and NaOH aq. solution (Fig. 5). The crystal morphologies for MIL-88B(Fe) and r-MIL-88(Fe) were similar in their shape and size, suggesting that TA/NaOH and $FeCl_3 \cdot 6H_2O$ recovered from the PET depolymerization process formed the well-defined MIL-88B(Fe) crystals. The XRD analysis of Fig. 5c also supports the identical crystal structures of MIL-88B(Fe) and r-MIL-88B(Fe) with distinct peaks at 9.2°, 10.1°, 10.6°, 16.7°, 18.1°, and 21.3°, corresponding to the (002), (100), (101), (103), (200), and (202) crystal planes, respectively.[56]

In Fig. 5d, the adsorption of RhB dye was compared for MIL-88B(Fe) and r-MIL-88B(Fe) samples. The comparable adsorption performances between the two samples, or slightly better adsorption performance of r-MIL-88B(Fe), confirms that r-MIL-88B(Fe) can be well applied as an adsorbent against a water-soluble pollutant. Fig. 5e shows the average pore diameter and specific surface area of the two MOF samples, which demonstrates that the pore characteristics of r-MIL-88B(Fe) are not inferior to those of MIL-88B(Fe); the data shows a slightly larger surface area for r-MIL-88B(Fe) than MIL-88B(Fe).

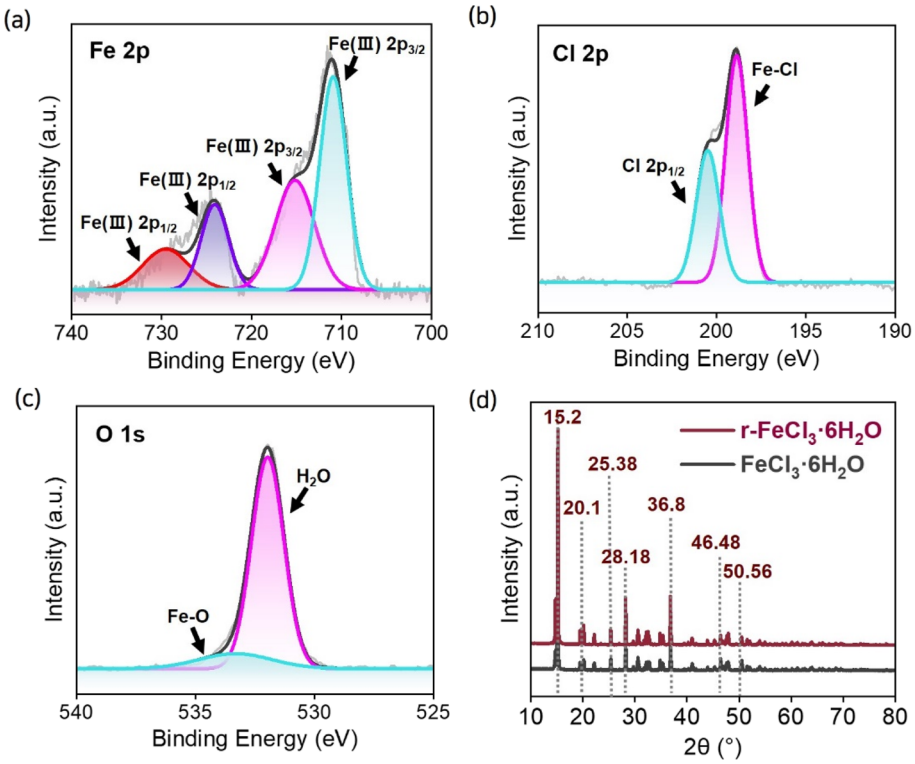

Fig. 4 (a–c) XPS spectra and (d) XRD patterns of the recycled $FeCl_3 \cdot 6H_2O$.

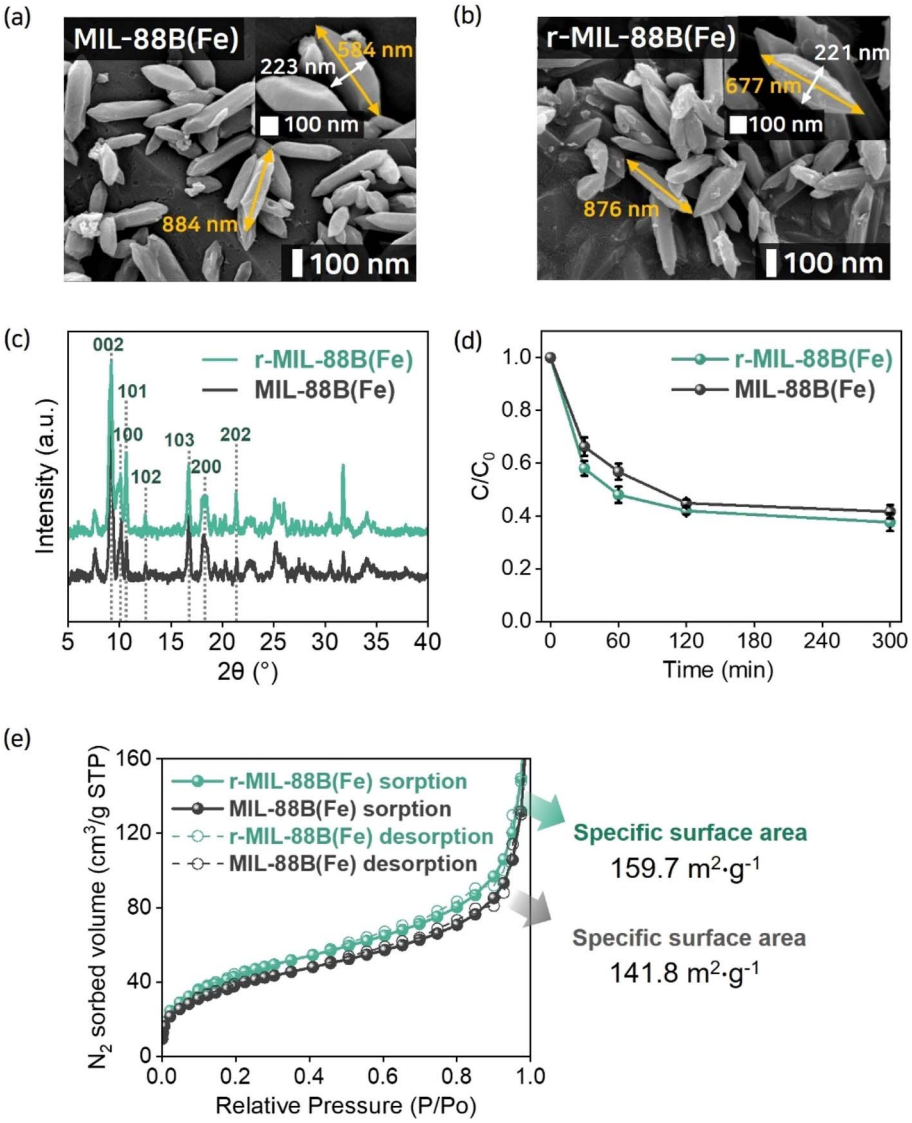

Fig. 5 SEM images of (a) MIL-88B(Fe) synthesized using recycled TA and $FeCl_3 \cdot 6H_2O$ and (b) r-MIL-88B(Fe) synthesized from commercially available compounds. (c) XRD patterns, (d) RhB adsorption performance, C is the dye concentration at a specific time (mg L^{-1}) and C_0 is the initial dye concentration (mg L^{-1}), (e) Brunauer–Emmett–Teller analysis of r-MIL-88B(Fe) and MIL-88B(Fe).

The results demonstrate that MIL-88B(Fe) was successfully synthesized using the TA/NaOH solution recovered from the developed process, without further purification steps for obtaining TA powder. Notably, $FeCl_3 \cdot 6H_2O$, one of the DES components, was obtained from the byproduct of the same depolymerization system, and it was recycled as a main component of MIL-88B(Fe) synthesis. To our knowledge, it is the first time to report that both MOF ingredients of metal and ligand components were simultaneously resourced from a single PET depolymerization system.

Recyclability of recovered dye

The recyclability of the dye obtained from the PET depolymerization reaction was investigated. Since the experiments were conducted on the discarded dyed fabrics, the chemical formula of the dye was unknown, except that PET is commonly dyed with azo- or anthraquinone-type dispersive dye. The recovered dye was dissolved in benzyl alcohol and was analyzed by FT-IR (Fig. 6a). The peaks were observed at: 1454 cm^{-1} corresponding to N=N stretching[57–59] a characteristic vibrational mode of azo compounds; and 1264 cm^{-1} for S–O stretching in the sulfonate group.[60] From the analysis, the dye recovered from the depolymerization process was characterized as a dispersive dye containing the azo and sulfite groups. To assess the recyclability of the recovered dye, the color difference between the PET fabric dyed with the recycled dye (noted as r-Dyed PET) and the discarded PET fabric originally dyed (noted as Discarded PET) was examined. Since the dyeing condition of the original fabric was unknown, the process conditions such as dye concentration, time, and temperature were arbitrarily adjusted to attain a similar color to the original fabric (Fig. S6†). From Fig. 6b, the CIE L^*, a^*, b^*, and the color difference value ($\Delta E \sim 1.4$) presented

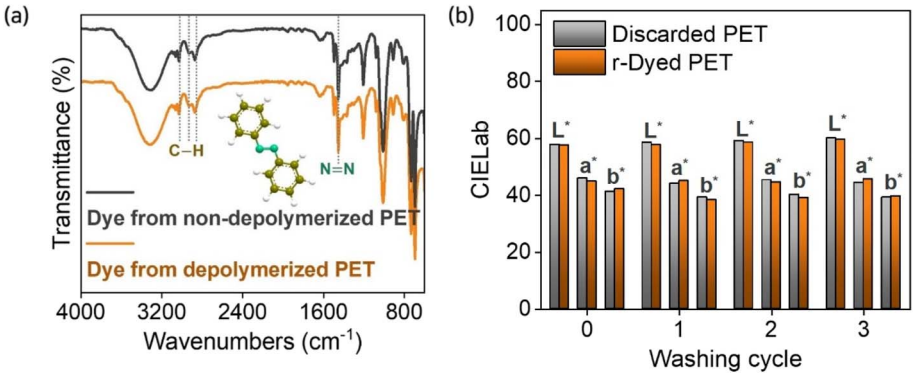

Fig. 6 (a) FT-IR analysis of recovered dye. (b) Comparison of *L**, *a**, *b** values between Discarded PET and r-Dyed PET.

the comparable color between the original fabric and the fabric treated with recycled dye, indicating the dye extracted from the depolymerization process can be effectively recycled for PET dyeing, as similar colors were maintained even after three washing cycles. The proposed dye recycling process minimizes the essential purification and separation steps required in previous studies, presenting a highly efficient method for recovering and recycling the dye through simple filtration during the waste recovery process.

To conclude, novel and efficient processes sequentially linked with PET depolymerization, byproducts recovery, and their recycling/upcycling were developed in this study. Applying the developed processes, PET was efficiently depolymerized at a lower reaction temperature than other hydrolysis processes, due to the synergistic catalytic effect of DES. From the recovery processes, TA/NaOH and $FeCl_3 \cdot 6H_2O$, the main ingredients of MIL-88B(Fe) synthesis, and the dye from the discarded PET fabric were appropriately recovered. The analytical results showed that all the recovered byproducts functioned well enough for proper MIL-88B(Fe) synthesis and PET fabric dyeing, demonstrating that the proposed process is a relevant option for circular practices of discarded PET textiles.

Life cycle assessment

LCA was performed on four case scenarios for our developed process including PET depolymerization (dep'n) and byproduct recovery. Case 1 analysis was conducted assuming that DES is not reused and all products (TA/NaOH(aq.), $FeCl_3 \cdot 6H_2O$, and dye) are intended products from this process, without giving any credits for the obtained products. From the life cycle impact analysis (LCIA), Case 1 recorded 13.62 kg CO_2 eq. of global warming potential (GWP), where the major causes for this value were: electricity (34.81%), PTSA (26.52%), and $FeCl_3 \cdot 6H_2O$ (23.76%) (Tables 2 and S7†).

Case 2 reflects the scenario where DES solvent/catalyst ($FeCl_3 \cdot 6H_2O$ and PTSA) is used two times, assuming that all DES is regained after the 1st dep'n process and a similar amount of DES is used in the 2nd dep'n. The analysis in Fig. 7 showed that GWP for Case 2 was 75% of Case 1, attributed to the full recycle of $FeCl_3 \cdot 6H_2O$ and PTSA. Since $FeCl_3 \cdot 6H_2O$ and PTSA were the major contributors to the environmental impacts, the reuse of DES (Case 2) significantly reduced the GWP. The analysis demonstrates that DES, simultaneously functioning as solvent and catalyst, needs to be reused as much as possible to reduce GWP, and an efficient solvent recovery process needs to be considered in developing an industrial-level process.

In Fig. 7, additional scenarios of Case 3 and Case 4 were analyzed, where the credits were given for the avoided production of virgin products. In Case 3, all the recovered materials (TA/NaOH, $FeCl_3 \cdot 6H_2O$, dye, and NaOH(aq.)) are recognized as useful byproducts, thus credits are given accordingly as it allows to avoid the production of virgin materials for TA/NaOH, $FeCl_3 \cdot 6H_2O$, dye, and NaOH(aq.) and to avoid the associated environmental burden as detailed in Table S3.† Case 4 considers the whole process as a TA production process, and the obtained byproducts except TA (that is, byproducts of $FeCl_3 \cdot 6H_2O$, dye, and NaOH(aq)) are considered as additional benefits, avoiding the production of $FeCl_3 \cdot 6H_2O$, dye, and NaOH(aq). Thus, in this case, credits are given to the avoided production of $FeCl_3 \cdot 6H_2O$, dye, and NaOH(aq.). Case 4 focuses on the TA production only to reflect the others' approach of using recycled TA only for MOF synthesis, even though our process and LCA does not include separation between TA and NaOH(aq.). From the analysis, Case 3 and Case 4 produced 79% and 94% of the GWP in Case 1, respectively. As the recovery of

Table 2 Contributes of the global warming potential in Case 1 analysis

Electricity and materials[a]	Contribution (%)
Electricity	34.81
PTSA	26.52
$FeCl_3 \cdot 6H_2O$	23.76
HCl	7.84
NaOH	4.30
Sorted waste PET	2.76
Water	0.02
Global warming potential	13.6242 kg CO_2-eq. (100%)

[a] As mentioned in ESI, since materials in the LCI DB (life cycle inventory database) were not exactly same concentration with our process, compensation value of water was added in the LCA to meet the total materials inserted.

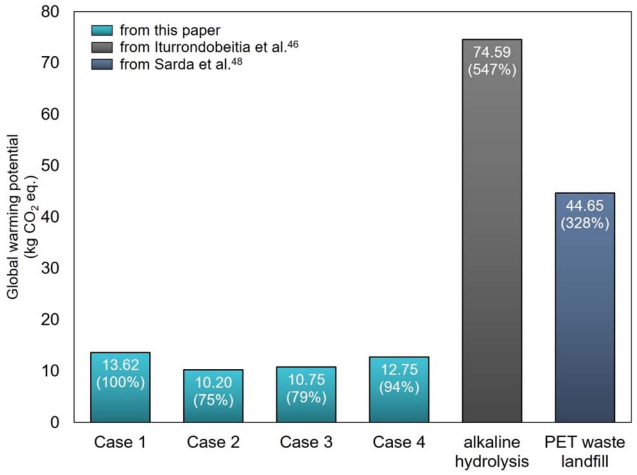

Fig. 7 Global warming potential of each scenario and referred methods. The relative impact ratio compared to Case 1 is presented in the parenthesis. Note. Iturrondobeitia *et al.*[30] also referred PET waste landfill data of Sarda *et al.*[62]'s study. Alkaline hydrolysis route's functional unit was 1 kg of as-received post-consumer PET, while our study used 1 kg of sorted waste PET. The functional unit of PET waste landfill was 1 kg of PET bottle.

TA was much larger than the other recovered materials, Case 3 showed significantly lower environmental impacts than Case 4. The analysis offers evidence-based justification for our efforts to recover TA and other byproducts for the maximized recycling of materials. Detailed data for other impact categories are summarized in Fig. S8.†

The scenarios from our developed process (Cases 1–4) were compared to other polyester depolymerization and waste PET handling methods for the GWP (Fig. 7). The compared data of alkaline hydrolysis was referred from Iturrondobeitia *et al.*[30] which used the same impact assessment method with this study (ReCiPe 2016(Hierarchist)). PET waste landfill was referred from other references,[61,62] and Iturrondobeitia *et al.*[30] also referred Sarda *et al.*[62] It should be noted that all data from Iturrondobeitia *et al.*[30] are the prospective LCA by the up-scale process while our results are calculated from the lab-scale process; the functional unit of Iturrondobeitia *et al.*[30] was 1 kg of as-received post-consumer PET, while our result was obtained from 1 kg of sorted waste PET. The functional unit of PET waste landfill was 1 kg of PET bottle. From Fig. 7, "alkaline hydrolysis" route which recovers TA like our study generated 74.59 kg CO_2 eq., which is much higher than any of the scenarios from our developed process. The "PET waste landfill" route showed 44.65 kg CO_2 eq., which was also much higher than our scenarios (Cases 1–4). This environmental impact analysis demonstrates the competitiveness of our depolymerization approach as a sustainable process, attributable to DES that allowed accelerated depolymerization by the effective catalytic action.

Conclusions

This study demonstrated an integrated framework for circular practices of PET textiles proposing an optimized recycling method and providing LCA validation. For depolymerization, a metal salt-based DES comprised of PTSA and $FeCl_3 \cdot 6H_2O$ was employed as both solvent and catalyst, and the reaction produced TA with a high yield of 95% in just 30 min at 100 °C. Sequential processes for multiple byproduct recovery were established, where the experimental approach emphasizes sourcing MOF ingredients of both metal and linker components from a single PET depolymerization reaction. The TA and $FeCl_3 \cdot 6H_2O$ regained from the depolymerization system were used to synthesize MIL-88B(Fe), which demonstrated an excellent adsorption performance against a water-soluble foulant, RhB. Furthermore, dye from the discarded PET fabric was also simultaneously recovered from the depolymerization system, and it was recycled for dyeing an uncolored PET fabric. Life cycle assessment (LCA) was performed on the varied scenarios of the developed process, and the results provided a solid ground to conclude that the developed process produced relatively less burden on the environment, attributed to the effective catalytic action of DES and the maximized use of byproducts. This work pioneers a comprehensive approach integrating novel experimental methods with LCA validation, establishing a novel proof-of-concept for maximizing the recycling potential of PET depolymerization byproducts. This work intends to demonstrate potential recovery processes for the materials that have been wasted or ignored before and their recyclability as useful materials, rather than testing the economic feasibility of recycling processes. Further study is suggested to examine the economic feasibility of the process with the recyclability of solvent and ethylene glycol. In response to the urgent need for sustainable practices for discarded textiles, this study provides insightful ideas on the circular development of value-added materials and suggests practical considerations for designing environmentally responsible processes.

Data availability

All data related to this publication are available either in the main manuscript or its ESI.†

Author contributions

Y. Woo and K. Baik designed and ran the experiments, analyzed the data, and wrote the original draft; S. Jeong ran the characterization experiments and analyzed the data; S. Lee and J. Kim analyzed the data and supervised the work. All authors reviewed and edited the manuscript.

Conflicts of interest

There are no conflicts to declare.

Acknowledgements

This work was supported by the National Research Foundation of Korea (NRF) grant funded by the Korea government (MSIT) (RS-2024-00405333; RS-2025-00523094).

References

1 Y. Peng, S. Sanati, A. Morsali and H. García, *Angew. Chem., Int. Ed.*, 2023, **62**, e202214707.
2 D. Chakraborty, A. Yurdusen, G. Mouchaham, F. Nouar and C. Serre, *Adv. Funct. Mater.*, 2023, **34**, 2309089.
3 H. D. Lawson, S. P. Walton and C. Chan, *ACS Appl. Mater. Interfaces*, 2021, **13**, 7004–7020.
4 D. A. Cabrera-Munguia, M. I. León-Campos, J. A. Claudio-Rizo, D. A. Solís-Casados, T. E. Flores-Guia and L. F. Cano Salazar, *Bull. Mater. Sci.*, 2021, **44**, 1–9.
5 Z. Li, L. Wang, L. Qin, C. Lai, Z. Wang, M. Zhou, L. Xiao, S. Liu and M. Zhang, *Chemosphere*, 2021, **285**, 131432.
6 N. Abigail K, J. Ronald T, M. Phillip J and S. Jin, *ACS Sustain. Chem. Eng.*, 2022, **11**, 18–22.
7 M. Jussara Lopes de, A. Tatiana Pereira de, N. João Mário Brito, S. Dejair de Pontes, C. Igor, S. Fernando, O. Suzane de Sant' Ana and M. Luiza Cristina de, *Sustainable Mater. Technol.*, 2023, **37**, e00689.
8 P. Marino, P. R. Donnarumma, H. A. Bicalho, V. Quezada-Novoa, H. M. Titi and A. J. Howarth, *ACS Sustain. Chem. Eng.*, 2021, **9**, 16356–16362.
9 R. Hardian, Z. Liang, X. Zhang and G. Szekely, *Green Chem.*, 2020, **22**, 7521–7528.
10 H. Li, J. Lei, L. Zhu, Y. Yao, Y. Li, T. Li and C. Qiu, *Green Energy Environ.*, 2024, **9**, 1650–1665.
11 M. Shanmugam, C. Chuaicham, A. Augustin, K. Sasaki, P. J. Sagayaraj and K. Sekar, *New J. Chem.*, 2022, **46**, 15776–15794.
12 S. Cheng, Y. Li, Z. Yu, R. Gu, W. Wu and Y. Su, *Sep. Purif. Technol.*, 2024, **339**, 126490.
13 Z. Cao, X. Fu, H. Li, S. Pandit, F. M. Amombo Noa, L. Öhrström, A. Zelezniak and I. Mijakovic, *ACS Sustain. Chem. Eng.*, 2023, **11**, 15506–15512.
14 P. Waribam, T. R. Katugampalage, P. Opaprakasit, C. Ratanatawanate, W. Chooaksorn, L. P. Wang, C.-H. Liu and P. Sreearunothai, *Chem. Eng. J.*, 2023, **473**, 145349.
15 C.-Y. Wang, H.-Y. Chu and C.-C. Wang, *Coord. Chem. Rev.*, 2024, **518**, 216106.
16 E. Barnard, J. J. R. Arias and W. Thielemans, *Green Chem.*, 2021, **23**, 3765–3789.
17 F. Cao, L. Wang, R. Zheng, L. Guo, Y. Chen and X. Qian, *RSC Adv.*, 2022, **12**, 31564–31576.
18 S. Javed, J. Fisse and D. Vogt, *Ind. Eng. Chem. Res.*, 2023, **62**, 4328–4336.
19 Z. Fehér, J. Kiss, P. Kisszékelyi, J. Molnár, P. Huszthy, L. Kárpáti and J. Kupai, *Green Chem.*, 2022, **24**, 8447–8459.
20 R. Sharma, H. Kumar, G. Kumar, S. Sharma, R. Aneja, A. K. Sharma, R. Kumar and P. Kumar, *J. Chem. Eng.*, 2023, **468**, 143706.
21 W. Chen, M. Li, X. Gu, L. Jin, W. Chen and S. Chen, *Polym. Degrad. Stab.*, 2022, **206**, 110168.
22 A. K. Nason, W. Phamonpon, T. A. Pitt, R. T. Jerozal, P. J. Milner, N. Rodthongkum and J. Suntivich, *Chem. Mater.*, 2024, **36**, 10319–10326.
23 R.-X. Yang, Y.-T. Bieh, C. H. Chen, C.-Y. Hsu, Y. Kato, H. Yamamoto, C.-K. Tsung and K. C.-W. Wu, *ACS Sustain. Chem. Eng.*, 2021, **9**, 6541–6550.
24 A. Khalid, S. Tahir, A. R. Khalid, M. A. Hanif, Q. Abbas and M. Zahid, *Green Chem.*, 2024, **26**, 2421–2453.
25 M. Rollo, F. Raffi, E. Rossi, M. Tiecco, E. Martinelli and G. Ciancaleoni, *Chem. Eng. J.*, 2023, **456**, 141092.
26 S. Marullo, C. Rizzo, N. T. Dintcheva and F. D'Anna, *ACS Sustain. Chem. Eng.*, 2021, **9**, 15157–15165.
27 M. M. Najafpour, *Acc. Chem. Res.*, 2022, **55**, 2260–2270.
28 K. Song, X. Qiu, B. Han, S. Liang and Z. Lin, *Environ. Sci. Nano*, 2021, **8**, 390–398.
29 W. T. Lang, S. A. Mehta, M. M. Thomas, D. Openshaw, E. Westgate and G. Bagnato, *J. Environ. Chem. Eng.*, 2023, **11**, 110585.
30 M. Iturrondobeitia, L. Alonso and E. Lizundia, *Resour. Conserv. Recycl.*, 2023, **198**, 107182.
31 Ü. Sibel, M. V. G. Kevin, D. Ruben, R. Martijn, M. Nicolas, R. Kim and D. M. Steven, *Green Chem.*, 2020, **22**, 5376–5394.
32 K. Leila, M. Arianna, S. Stefania, E. H. Nissrine, M. Pascale and R. Julien, *Mater. Adv.*, 2021, **2**, 2750–2758.
33 W. Yang, J. Wang, L. Jiao, Y. Song, C. Li and C. Hu, *Green Chem.*, 2022, **24**, 1362–1372.
34 M. Rollo, M. A. Perini, A. Sanzone, L. Polastri, M. Tiecco, A. Torregrosa-Chinillach, E. Martinelli and G. Ciancaleoni, *RSC Sustainability*, 2024, **2**, 187–196.
35 T. Cai, H. Du, X. Liu, B. Tie and Z. Zeng, *Environ. Technol. Innov.*, 2021, **24**, 102031.
36 H. Lin, S. Bean, M. Tilley, K. Peiris and D. Brabec, *Food Anal. Methods*, 2021, **14**, 268–279.
37 T. H. Nguyen and K.-Y. Chiang, *Sustain. Environ. Res.*, 2024, **34**, 16.
38 V. Țucureanu, A. Matei and A. M. Avram, *Crit. Rev. Anal. Chem.*, 2016, **46**, 502–520.
39 Y. Ko, T. J. Azbell, P. Milner and J. P. Hinestroza, *Ind. Eng. Chem. Res.*, 2023, **62**, 5771–5781.
40 Y. Li, H.-Y. Bi, Y.-S. Jin and X.-Q. Shi, *RSC Adv.*, 2014, **4**, 58307–58314.
41 R. Chu, Y. Zhang, T. Xing and G. Chen, *RSC Adv.*, 2020, **10**, 42633–42643.
42 J. H. Braun, A. Baidins and R. E. Marganski, *Prog. Org. Coat.*, 1992, **20**, 105–138.
43 X. Lv, B. Yan, Y. Shao, H. Zhang, H. Zhang and J. Zhu, *Particuology*, 2022, **67**, 18–26.
44 U. Gesenhues, *J. Photochem. Photobiol., A*, 2001, **139**, 243–251.
45 M. Salmanion and M. M. Najafpour, *J. Phys. Chem. C*, 2023, **127**, 18340–18349.
46 W. Yang, Z. Mei, S. Feng, C. Li, J. Guo, H. Bian, H. Xiao, H. Dai, C. Hu and J. Han, *ACS Sustain. Chem. Eng.*, 2023, **11**, 10172–10182.
47 Z. Xu, S. Gu, Z. Sun, D. Zhang, Y. Zhou, Y. Gao, R. Qi and W. Chen, *Environ. Sci. Pollut. Res.*, 2020, **27**, 11012–11025.
48 Z. Hou, P. Yan, B. Sun, H. Elshekh and B. Yan, *Results Phys.*, 2019, **14**, 102498.
49 L. Wei, Y. Zhang, Y. Yang, M. Ye and C. C. Li, *Small*, 2022, **18**, 2107667.

50 D. Pradhan and K. Leung, *J. Phys. Chem. C*, 2008, **112**, 1357–1364.
51 Y. Jiang, M. Dai, F. Yang, I. Ali, I. Naz and C. Peng, *Water*, 2022, **14**, 894.
52 H. S. Casalongue, S. Kaya, V. Viswanathan, D. J. Miller, D. Friebel, H. A. Hansen, J. K. Nørskov, A. Nilsson and H. Ogasawara, *Nat. Commun.*, 2013, **4**, 2817.
53 N. Louvain, A. Fakhry, P. Bonnet, M. El-Ghozzi, K. Guérin, M.-T. Sougrati, J.-C. Jumas and P. Willmann, *CrystEngComm*, 2013, **15**, 3664–3671.
54 Z. Wang, Y. Jin, Y. Wang, Z. Tang, S. Wang, G. Xiao and H. Su, *ACS Sustain. Chem. Eng.*, 2022, **10**, 7965–7973.
55 S. Shirazimoghaddam, I. Amin, J. A. Faria Albanese and N. R. Shiju, *ACS Eng. Au*, 2023, **3**, 37–44.
56 M. Ma, A. Bétard, I. Weber, N. S. Al-Hokbany, R. A. Fischer and N. Metzler-Nolte, *Cryst. Growth Des.*, 2013, **13**, 2286–2291.
57 H. Shaki, K. Gharanjig and A. Khosravi, *Biotechnol. Prog.*, 2015, **31**, 1086–1095.
58 A. Mohammadi, M. R. Yazdanbakhsh and L. Farahnak, *Spectrochim. Acta, Part A*, 2012, **89**, 238–242.
59 N. Biswas and S. Umapathy, *J. Phys. Chem. A*, 2000, **104**, 2734–2745.
60 S. Ramesh and L. J. F. Yi, *Ionics*, 2009, **15**, 413–420.
61 A. Ncube and Y. Borodin, *7th International Forum On Strategic Technology (IFOST) 2012*, 2012, pp. 1–6.
62 P. Sarda, J. C. Hanan, J. G. Lawrence and M. Allahkarami, *J. Polym. Sci.*, 2022, **60**, 7–31.